

Carbon Aerogels: a study with different models of the effect resorcinol/catalyst at different ratios after pyrolysis and the effect on textural properties

Rafael Alberto Fonseca-Correa ¹, Marlon Jose Bastidas-Barranco ²,
Liliana Giraldo ³ and Juan Carlos Moreno-Piraján ^{1,*}

¹ Facultad de Ciencias, Departamento de Química, Grupo de Investigación en Sólidos Porosos y Calorimetría, Universidad de los Andes, Bogotá, 11001000, Colombia

² Facultad de Ingeniería, Grupo DestaCar, Universidad de la Guajira, Guajira, 440001, Colombia

³ Facultad de Ciencias, Departamento de Química, Universidad Nacional de Colombia, Bogotá, 11001000, Colombia

* Corresponding author at: Facultad de Ciencias, Departamento de Química, Grupo de Investigación en Sólidos Porosos y Calorimetría, Universidad de los Andes, Bogotá, 11001000, Colombia.

Tel.: +57.1.3394949 (ext. 2786). Fax: +57.1.3324366. E-mail address: jumoreno@uniandes.edu.co (J.C. Moreno-Piraján).

ARTICLE INFORMATION



DOI: 10.5155/eurjchem.8.3.279-287.1593

Received: 03 June 2017

Received in revised form: 31 July 2017

Accepted: 05 August 2017

Published online: 30 September 2017

Printed: 30 September 2017

KEYWORDS

QSDFT

NLDFT

Aerogels

Surface chemistry

Adsorption properties

Microporous materials

ABSTRACT

Eight samples of carbon aerogels were prepared at various resorcinol/catalytic (R/C) ratios (ranging from 25 to 1500) and followed the changes in structure after pyrolysis. Isotherms of N₂ to 77 K were determined to calculate the textural parameters using Dubinin-Astakhov (DA), Barret Joyner and Halenda (BJH), Non-Local Density Functional Theory (NLDFT) and Quenched Solid Density Functional Theory (QSDFT) models. The results generated two series of samples. In series I, a single type of pores developed (microporous, at low R/C weight ratio). Series II developed mesoporosity to top gears of R/C (> 400). The specific areas ranged from 64 to 990 m²/g. Additional models were applied to the materials synthesized, which allowed for adjustment to a system of "cylinder-slit" pores by applying the QSDFT kernel, with an error percentage ranging from 0.03 to 0.74.

Cite this: *Eur. J. Chem.* 2017, 8(3), 279-287

1. Introduction

There have been reports of solids prepared with different porosity, with the objective of find a solution at the different types of environmental problems such as: decontamination of water, the reduction of particulate matter in the air, storage of gases etc. Within these solids may be mentioned activated carbon, carbon cloths, zeolites and silica's among others. Carbon aerogels are a series of special materials that were synthesized for the first time in the decade of the 30's, and subsequently developed exponentially by their wide applications. These materials have great effect today for their textural and chemical characteristics; since it is possible to control these properties during their synthesis; it is possible to obtain aerogels with high porosity [1]. Some properties of these solids are related to the very particular structure obtained through the control of the variables during the synthesis process, and of these properties will depend its possible final applications. The porous structure in these materials is generated during the sol-gel process synthesis, in which there is a

growth of the polymeric chains from a chemical solution, and then the organization of the monomer units occurs with the formation of the polymer network. Initially an addition reaction occurs between resorcinol and formaldehyde forming the monomer units, followed by a condensation and polymerization step Figure 1 [2-5].

Then drying is performed under supercritical conditions allowing slowly remove the solvent to prevent the gel from collapsing due to the surface tension of the liquid during the evaporation process. The mesoporous structure is affected by the applied drying method, and the microporosity does not depend on the drying processes. Previous treatments with exchange of water per acetone prevent the collapse of the structure [6]. In the synthesis developed by Pekala *et al.* [2-4], different types of carbon gels have been developed under different synthesis conditions, porous carbon gels have been used according to their textural properties for various applications such as electronic components, photoconductors, gas separation systems among other applications [2-4].

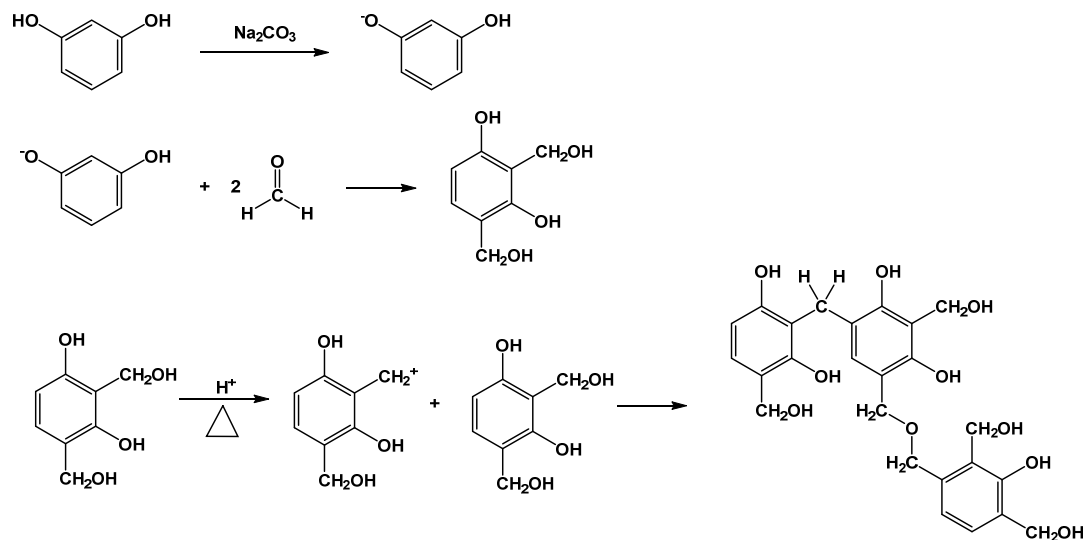


Figure 1. Reaction of polymerization between the resorcinol and formaldehyde in the presence of the catalyst Na_2CO_3 [adapted from Lin C., Ritter J.A., Effect of synthesis pH on the structure of carbon xerogels, Carbon, 1997, 35, 1271-1280] [5].

One of the main application areas of carbon aerogels is adsorption. Due to their high surface area and facility of control of pore size distribution, these materials can be considered as good adsorbents, which can be characterized by their adsorption capacity of different compounds [7-9]. For this reason, these properties are related to the conditions of synthesis and processing, being possible the synthesis of a greater variety of materials that have unique characteristics. At present, resorcinol formaldehyde carbon gels have been produced with different variations but following the same original recipe [10-12]. On the other hand, of many similar statements that can be found in the literature, there are still no reports on the implementation of aerogels in the large-scale adsorption process [13,14].

The carbon aerogel consist of a three-dimensional network structure made of carbon spherical nodules uniforms interconnected, in which according to the scientific literature the pores are predominant mesoporous, although according to the preparation method can be generated micropores, which are likely to have importance in the final properties of the carbon aerogels. Several authors [15-21] have conducted studies to evaluate adequately and systematically porosity that develops in carbon materials by different methods, including the effect pore subtraction method (SPE) using the graphics high α_s resolution, for N_2 adsorption isotherms at 77 K by which they can properly evaluate the structure of micropores [15,19]. According to these authors, to apply the analysis of high-resolution α_s it is possible to find adequate information on the microporosity developed in the process of synthesis of aerogels, as well as of the mesoporosity [22] that are in good agreement with other methods that have been used for several decades [23-25].

The smooth-surfaced in carbon aerogels are found whose size decreases with increased cross-linking in the gel precursor. The morphology is controlling by dominant process in phase separation that restricted to nanometer size scales by polymer cross-linking [26]. Different technics were used to corroborate this, pore analysis of small-angle X-ray scattering results was used to study the structure of aerogels, and it is concluded that the aerogels structure is formed from nanoscale phase separation in the initial solution and show that the cross-link density controls both the size and the skeletal density of the material [27]. Thus, the influence of physical and chemical properties of carbon aerogels is possible

to use to develop supported heterogeneous catalysts to obtained non-graphitic (amorphous) materials, because the high dispersion of an active phase is highly influenced by the porosity and surface area of the support (PSD). The presence of a large mesopore volume that is one characteristic from carbon aerogels, was suggested as an important factor to prepare highly dispersed catalysts, which are now necessary for some applications [28]. Another aspect to take in account is the gelation time that depend on the nature of the carbonate used how catalyst, because is defined during this stages the porosity of the samples when is formed the primary particles. If the counter-ion size of the carbonate used is increasing, mesoporous change to microporous in the carbon aerogels structure, and is denser. If the catalyst was acid only increased and widened the microporosity, but do not affect the mesoporosity [29,30].

In this research, carbon aerogels were synthesized with various resorcinol/catalyst relationships to systematically study the effect of the catalyst on the morphology for a given R/C as a function of the textural structure from the analysis results, which were obtained. We are used Barrett-Joyner-Halenda (BJH) [31], Dubinin-Astakhov (DA) method [32], recent models Non-Local Density Functional Theory (NLDFT) and Quenched Solid State Functional Theory (QSDFT) [33-36].

2. Experimental

2.1. Synthesis of the organic aerogels

The carbon aerogel synthesized in this research were prepared using the method described by Pekala *et al.* widely in the literature [2-4] with some slight modifications in the quantities of reagents, using the method of polymerization sol-gel with monomers resorcinol and formaldehyde (R and F) with sodium carbonate as catalytic converter (C) [37].

For obtaining the wet gels of resorcinol-formaldehyde is used resorcinol (R) (98% pure), formaldehyde (F) (solution to 37%), Na_2CO_3 (99.9% purity), all trademark Aldrich™, and deionised water. The resorcinol (0.1120 moles) was dissolved in deionised water (W) to a constant relationship (R/W (0.075)). Below is added Na_2CO_3 (C) in different proportions (R/C): 25, 50, 100, 200, 400, 600, 800 and 1500, which acts as a catalyst for the reaction (basic catalyst) to accelerate the dehydrogenation of resorcinol.

Table 1. Textural parameters of aerogels [37].

Sample	S_{BET} [m ² /g]	D-A				B-J-H	
		$V_{micropore}$ [cm ³ /g]	E_0 [kJ/mol]	n	Pore radio [Å]	V_{meso} [cm ³ /g]	Pore radio [Å]
AeW25	64	0.02	8.06	2.7	7.1	0.01	23.1
AeW50	196	0.07	6.89	3.4	7.5	0.02	18.2
AeW100	295	0.11	8.11	2.2	7.0	0.02	18.2
AeW200	478	0.18	8.00	2.2	7.0	0.02	18.1
AeW400	609	0.24	8.57	1.8	6.8	0.18	18.4
AeW600	849	0.33	8.15	1.8	6.9	1.23	79.3
AeW800	876	0.34	8.26	1.8	6.9	1.28	79.3
AeW1500	990	0.36	8.15	2.4	7.0	0.31	18.2

The formaldehyde solution was added on the solution of resorcinol (R/F = 0.5) and was subjected to vigorous agitation. Followed the solutions are placed in well-closed glass moulds (7 cm in length × 1 cm internal diameter) and were cured: 1 day at 25 °C, 2 days at 50 °C and 3 days at 70 °C. The gels of resorcinol-formaldehyde (R/F) resulting were washed with ethanol followed by washing with acetone, and subsequently dried with CO₂ under conditions supercritical (38-40 °C, 90-100 atm), obtaining in this way the respective aerogels resorcinol-formaldehyde (R/F). The organic aerogel synthesized were pyrolyzed well in an atmosphere of N₂ over the course of 3 hours at a heating rate of 5 °C/min, which brought samples to a temperature of 850 °C in an oven (Carbolite MFT Type 12/38/400), so as to obtain the carbon aerogel [37].

In order to obtain the carbon aerogel with a different porosity used a wide range of the resorcinol/catalytic (R/C) relations, as was described in our work previously [37]. The synthesized samples in this research are called: AeW25, AeW50, AeW100, AeW200, AeW400, AeW600, AeW800 and AeW1500 where the last numbers refer to the R/C ratio [37].

2.2. Porous characterization of R/F carbon aerogels

The study of the textural properties of the carbon aerogel synthesized in this research was evaluated from nitrogen adsorption-desorption isotherm that are determined to -196 °C. The analysis of adsorption was made in a sortometer IQ₂ Quantachrome Inc. (Boynton Beach, Miami, FL) to conduct the study of the microporosity and mesoporosity. Before the measurement of adsorption isotherms of samples, these were heated overnight at 250 °C and 50 millitorr vacuum to remove adsorbed species. Several models were used to investigate the effect of the catalyst on the textural properties of carbon aerogels. Among these models were used Brunauer-Emmett-Teller (BET) [38-43], Dubinin-Astakhov (DA) [32,44], the Barret, Joyner and Halenda (BJH) [31] and density functional theory (DFT) [33-37].

The volume of the primary micropores (< 0.7 nm) was determined by the application of Dubinin-Astakhov (DA) equation [25,32,44] that corresponds to the volume adsorbed to the $(P/P^0) = 0.1$ as well as the distribution of pore size. The mesopores volume (V_{mes}) was calculated as the difference between the volume of nitrogen adsorbed to the $(P/P^0) = 0.95$ and $(P/P^0) = 0.10$. The apparent specific surface area was evaluated from the BET method with the data obtained to relative pressures (P/P^0) between the ranges 0.04-0.35. The distribution of pore size (PSD) was calculated through methods corresponding to the theories density functional non-local (NLDFT) and the quenched solid (QSDF) assuming cylindrical models, slit and combined (cylindrical and slit) for the pores of the materials [33-37]. These models are based on thermodynamic arguments which gives them a plus when being employed; The calculation of the pore size distribution is based on a solution of the generalized adsorption equation (GAE), which is sometimes also called the integral adsorption equation, as shown in the following Equation (1), which correlates the kernel of theoretic isotherms with the experimental isotherm of adsorption (or desorption).

$$N_{exp}\left(\frac{P}{P^0}\right) = \int_{D_{min}}^{D_{max}} N_{QSDF}\left(\frac{P}{P^0}, D\right) f(D) dD \quad (1)$$

Here, $N_{exp}(P/P^0)$ represents an experimental adsorption isotherm; D_{min} and D_{max} are the minimum and maximum pore sizes in the kernel. The kernel $N_{QSDF}((P/P^0), D)$ represents a set of theoretical isotherms in model pores for a series of pore diameters (D), which cover the whole range of micro and mesopores accessible in the adsorption experiment [45].

3. Results and discussion

3.1. Analysis of adsorption isotherms of N₂ at 77 K

The structures obtained in this work consisted in granular type gels are constituted by spherical-like nodules between 1 and 2 mm. Nitrogen adsorption-desorption isotherm, from the corresponding carbon aerogel synthesized in this investigation are shown in Figure 2a and 2d. These are very useful for the characterization of solid regularly organized as in the case of materials of this research. The change in the structure of aerogels prepared in this work can be seen by analysing of the nitrogen adsorption isotherm, and the corresponding calculated parameters for the porosity which are reported in Table 1, that correspond to the textural parameters obtained by applying D-A and BJH models. Table 2 shows the errors of the pore distribution by applying the NLDFT and QSDF methods. The textural properties of solids synthesized are showed, which were determined by performing a detailed analysis of each of the nitrogen adsorption isotherms at -196 °C, using models reported in the scientific literature to analyse the effect of the R/C ratio in each aerogel. The results show two behaviours very marked: a series of aerogels (Ae25, AeW50, AeW100 and AeW200), which we will call hereinafter series I, which has a predominant development of micropores. A second series of aerogels, which call on later series II (AeW400, AeW600, AeW800 and AeW1500), where the effect of the ratio R/C is manifested in the appearance of mesopores.

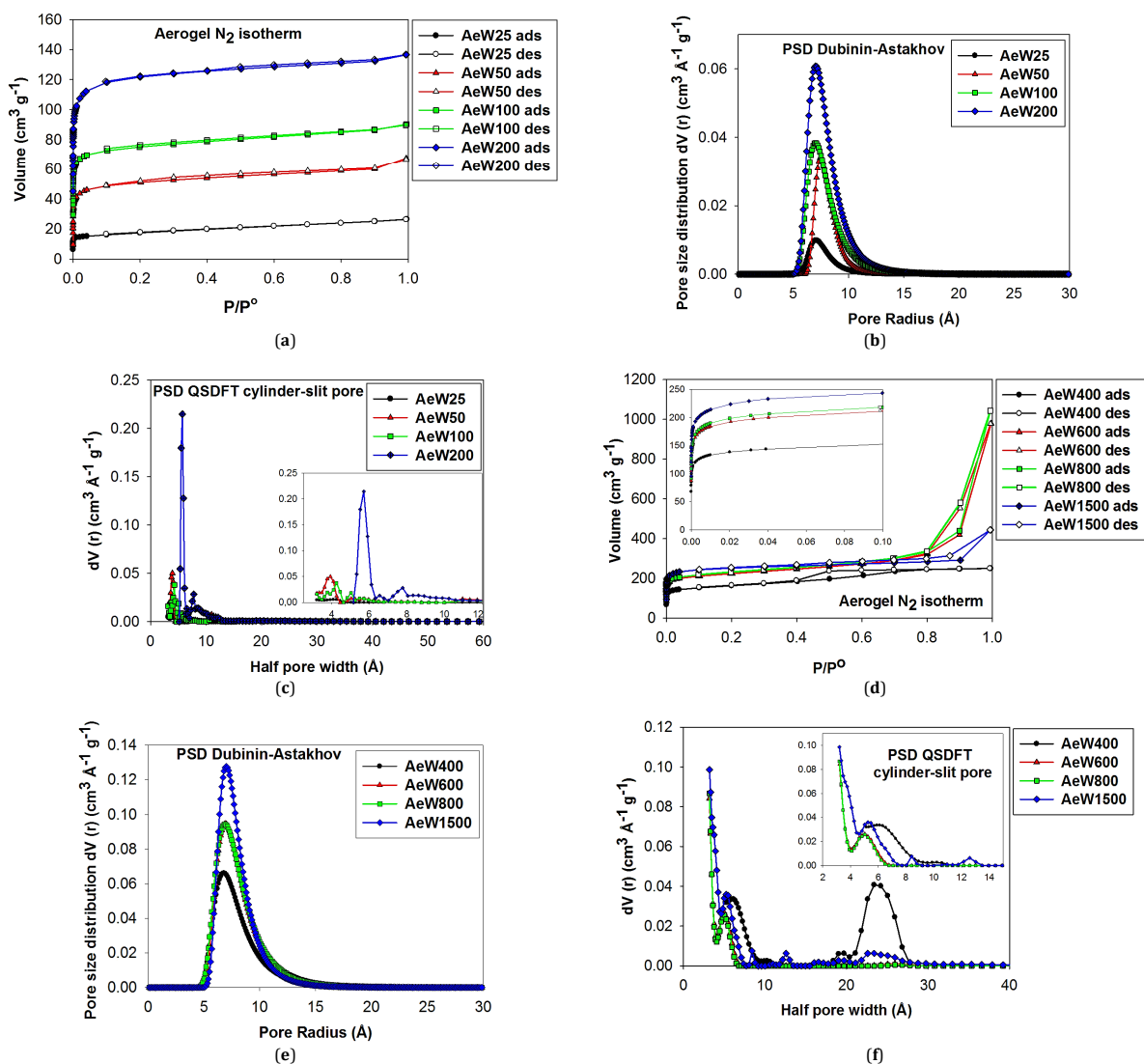
Nitrogen adsorption isotherms at -196 °C corresponding to the series I are shown in Figure 2a; these correspond to type I isotherms according to the classification of IUPAC isotherms [22,46] characterized by having a well-developed pore system and particularly high micropores.

The isotherms obtained for the aerogels series I, synthesized at these R/C ratios in this research are reversible and have not hysteresis loop, characterized by presenting a plateau well defined and parallel to the axis of relative pressure. A slight gap occurs in the AeW100 and AeW200 samples without such separations can be called hysteresis loop. It is probable that these small separations should incipient development to of mesoporosity, given that has been increased to R/C ratio and that is associated with the reaction between resorcinol and Na₂CO₃, with the first step corresponding of the addition reaction.

The resorcinol (1,3-dihydroxybenzene) is a trifunctional phenolic compound which is capable of adding formaldehyde at positions (2,4,6) of the aromatic ring.

Table 2. Aerogels pore size distribution NLDFT-QSDFT, fitting error [37].

Samples	Pore volume cyl [cm ³ /g]	Average width of pore cyl [Å]	E [%]	Pore volume cyl-slit [cm ³ /g]	Average width of pore cyl-slit [Å]	E [%]	Pore volume slit [cm ³ /g]	Average width of pore slit [Å]	E [%]
NL-DFT									
AeW25	0.04	5.8	0.47	0.04	3.1	3.60	0.04	3.6	0.76
AeW50	0.10	5.8	0.72	0.10	3.1	0.35	0.09	4.1	0.58
AeW100	0.13	5.8	0.27	0.13	3.1	0.15	0.13	3.6	0.68
AeW200	0.21	5.8	0.26	0.21	3.1	0.10	0.19	3.6	0.73
AeW400	0.38	5.2	0.23	0.38	3.1	0.23	0.36	3.6	1.13
AeW600	1.24	7.4	3.94	1.23	3.5	3.80	1.24	3.6	1.13
AeW800	1.32	7.4	4.00	1.31	3.5	3.89	1.33	3.6	1.14
AeW1500	0.62	5.8	1.02	0.61	3.1	1.07	0.60	3.6	0.70
QS-DFT									
AeW25	0.04	5.5	0.24	0.04	4.1	0.18	0.04	3.1	0.32
AeW50	0.09	6.3	0.99	0.09	3.9	0.07	0.09	3.9	0.23
AeW100	0.13	5.7	0.05	0.13	4.3	0.04	0.13	3.1	0.12
AeW200	0.20	5.7	0.04	0.19	4.3	0.03	0.20	3.1	0.11
AeW400	0.37	23.4	0.40	0.36	23.4	0.40	0.36	3.1	0.62
AeW600	1.27	5.7	0.71	1.27	3.2	0.70	1.24	3.1	1.54
AeW800	1.36	5.3	0.73	1.35	3.2	0.74	1.32	3.1	1.57
AeW1500	0.61	5.5	0.22	0.61	3.2	0.17	0.60	3.1	0.57

**Figure 2.** Nitrogen adsorption isotherms on carbon aerogels at -196 °C, PSD Dubinin-Astakhov and PSD QSDFT applied cylinder-slit pore model. (a) Isotherms AeW25, AeW50, AeW100, AeW200, with N₂ at -196 °C; (b) PSD applied Dubinin-Astakhov model: AeW25, AeW50, AeW100, AeW200; (c) PSD applied QSDFT cylinder-slit pore: AeW25, AeW50, AeW100, AeW200; (d) Isotherms AeW400, AeW600, AeW800, AeW1500 with N₂ at -196 °C; (e) PSD applied Dubinin-Astakhov model: AeW400, AeW600, AeW800, AeW1500; (f) PSD applied QSDFT cylinder-slit pore: AeW400, AeW600, AeW800, AeW1500 [37].

This phase synthesis is favoured at alkaline pH, because it allows anion generation resorcinol to promote the formation of hydroxymethyl monomers, Figure 1. From the thermodynamic point of view, the anions of resorcinol are much more active than molecules resorcinol uncharged, which allows subsequently the hydroxymethyl compounds that will generate the monomers, which polymerize to give the final organic gel form. The phase II presents the condensation reaction corresponding of hydroxymethyl derivatives formed in phase I. In this condensation reaction, the methylene and ether-type bonds between the various hydroxymethyl groups that originate the polymer are generated. With the progress of the reaction, the crosslinking of aggregates occurs to form a fully interconnected structure. When using high concentrations of catalyst, i.e. to basic pH above 9, phase I of adding or nucleation is more favoured, producing polymeric nodules smaller and more interconnected among themselves. This is consistent with the results found in this research and with the reaction proposal in the literature, because as can be seen in the Table 1, when increases the ratio R/C (more basic character) after the pyrolysis and obtain carbon aerogels. The specific surface areas and the radius and volumes of pores in general increase, which is directly related with the structure previously generated during the polymerization process [37].

Parameters D-A show that micropore volume increasing as a function of R/C ratio, while the pore radius remains relatively constant for each of the samples at the prepared relations (series I and series II), around 7 Å, while "n" has a value of approximately 2.0, which is associated with and corresponds to carbonaceous materials. It is demonstrating in this case that carbon aerogels synthesised in this work possess a porous network system that conform to those with activated carbons. Values characteristic of energy obtained are approximately 8.0 kJ/mol, which allows one to deduce that the order of magnitude of carbon aerogels synthesised has adequate potential to adsorb the nitrogen molecules.

Figures 2b, 2c, 2e and 2f show the PSD initially calculated by the D-A model, further detailed studies were conducted using the algorithms corresponding to NLDFT and QSDFT for series I and II; the results are slightly different (only distributions are shown with the QSDFT because they are adjusted better). As can be seen the pore radius calculated by D-A is approximately 7 Å presenting monomodal curves, well-defined and narrow, characteristics of microporous solids, while with the NLDFT model the average width of pore is approximately 3.1 Å and with the QSDFT the average width of pore is approximately 4 Å, which is also within the range of microporous materials. These results are consistent with the shape of the nitrogen adsorption isotherms obtained for this series, which as mentioned before, correspond to fundamentally microporous materials. Additionally, the Table 1 also shows the mesopore volumes (V_{meso}) calculated from BJH method [24]. The other hand in Table 2 the volumes assuming cylindrical pores, slit pores and cylindrical-slit, using the NLDFT and QSDFT [33-37] kernels are also presents and the calculated errors expressed as error percentages of these (E%) for this model.

The PSD and radius of the pores corresponding to BJH are not shown in this work, because despite being calculated with the branch of adsorption, has been amply demonstrated in the scientific literature that this method underestimates the pore size, because the equation of Kelvin, theory on which this model is based, it ignores the adsorbent-adsorbate interactions. The most recent developments to correct this deviation is based on the NLDFT [33,37].

Volumes found by the methods: DA, BJH and NLDFT and QSDFT models are consistent with those found using other models for series I, where there is no presence of mesoporosity, but correspond to samples mainly microporous, which was expected according to the shape of the isotherms

and similarities between the values obtained for the pore volume obtained by these methods.

In contrast, the series II, where the ratio R/C increases strongly, presents a development of mesoporosity whose values are between 0.18-0.36 cm³/g. An interesting aspect of this research was to apply the models QSDFT and NLDFT and compare the results obtained from these, particularly in what refers to the volumes of pores obtained with different models as mentioned before. When comparing the results obtained for these volumes, which fit better correspond to the model for pores cylindrical-slit by applying the model QSDFT, this both for the series I and II.

This difference in the results obtained explains, taking into account the thermodynamic postulates on which each of the models have been developed. The NLDFT model was designed for solids organized, so that when applied in materials disorganized adjustment is not adequate. Today, the applications of this model for materials not-organized are based on the existence of a network of pores smooth and homogeneous, so do not need consideration the heterogeneity energy and geometry that possess such materials. The NLDFT model works with fluids within pores with a given geometry (cylinders, spheres and slits), being a one-dimensional character model, which assumes a thermodynamic potential in the solid-liquid interface and the density of the liquid, which varies only in direction normal to the wall of the pore. However, in carbonaceous materials disorderly, as is the case of this research, carbon aerogels, the transition that occurs between layers occurs due to the heterogeneities and geometry energetics of real surfaces. This approach generates jumps transition layers in the theoretical isotherms, causing artificial gaps in the pore distributions calculated. This deficiency NLDFT dimensional model has been reported and investigated extensively in the scientific literature [33,37].

On the other hand, the QSDFT adsorption model in heterogeneous materials is based on a parameter of surface roughness [33,34]. QSDFT is a model of DFT (Density Functional Theory) multicomponent, where the solid is treated as one of the components of the adsorbate-adsorbent system. The authors that proposed this model, them say that in contrast to the traditional model NLDFT, which assumes the walls of the pores with graphitic structure, in the QSDFT model the solids is modelled using the distribution of solids atoms instead of the external surface potential. Thus, the QSDFT model considers the effect of the heterogeneity of the surface, where this heterogeneity is characterized here by an only roughness parameter that represents the scale of the undulation characteristic of the surface. This model considers the solid-fluid and fluid-fluid interactions are divided into areas that are repelled and which parts are attracted to the surface. The interactions of the spheres are treated with the basic theory of multicomponent measurement (FMT fundamental measure multicomponent theory) [33,36]. The density distribution of solid introduced into the QSDFT model to take account of the surface roughness eliminates the strong interactions between the layers of fluid near the walls while the effect of the microporosity of the pore walls can be naturally incorporated in the model using a reduced density solid.

The main feature of the QSDFT model is that it quantitatively considers the geometric heterogeneity of the surface by the roughness parameter [33-37]. This roughness parameter represents half the width of extension level of surface molecular waviness of pore walls. In general, this modelling depends on the origin of the porous material, the synthesis process and the degree of carbonization and chemical activation. The roughness parameter can be determined by comparison of theoretical and experimental adsorption isotherm of a reference surface, and can be calculated for a specific type of material.

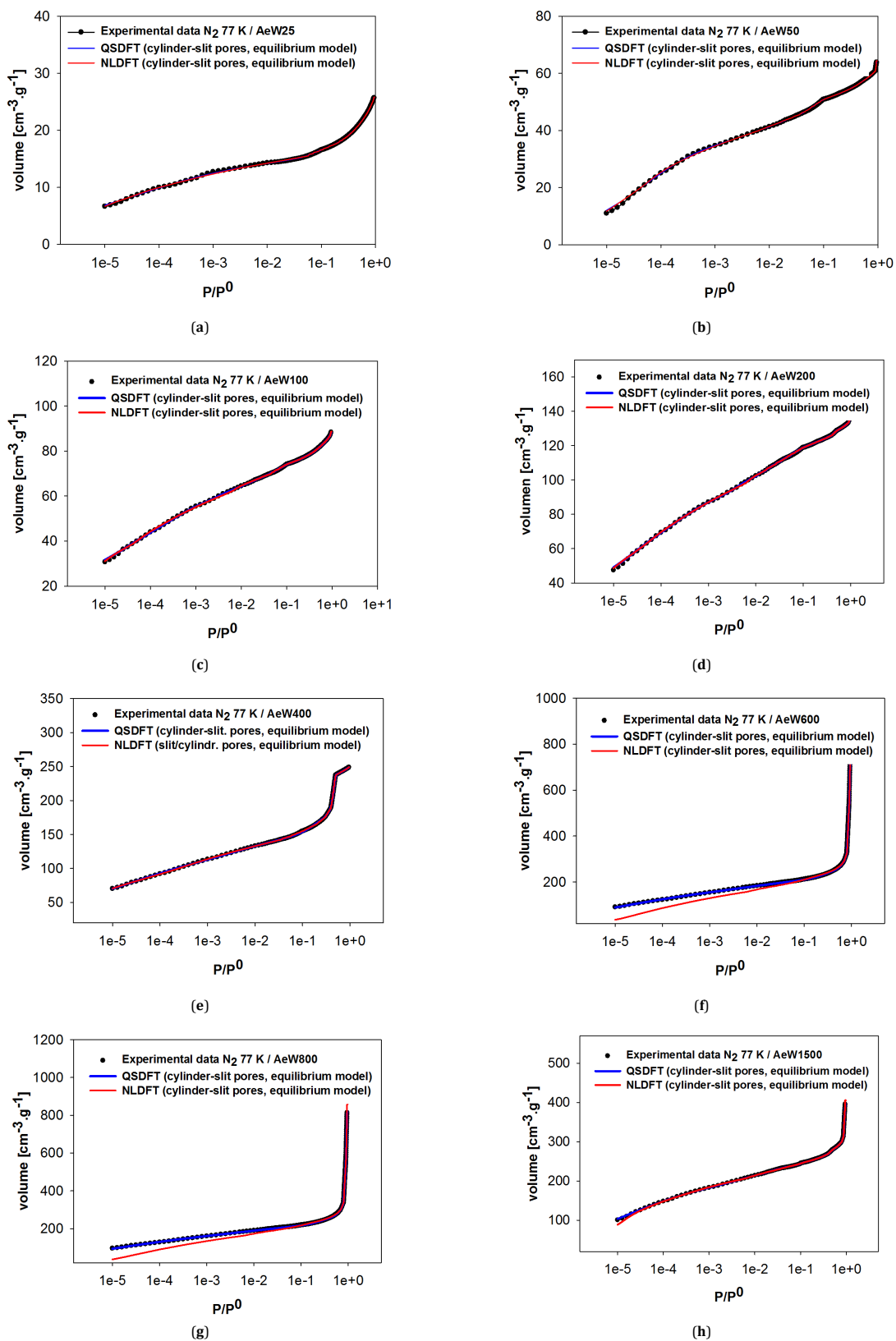


Figure 3. Comparison of the QSDFT and NLDFT methods for nitrogen adsorption for the carbon aerogels. Experimental isotherms and fit from NLDFT and QSDFT plotted logarithmically (semi-scale) using a kernel cylindrical-slit. (a) AeW25; (b) AeW50; (c) AeW100; (d) AeW200; (e) AeW400; (f) AeW600; (g) AeW800; (h) AeW1500.

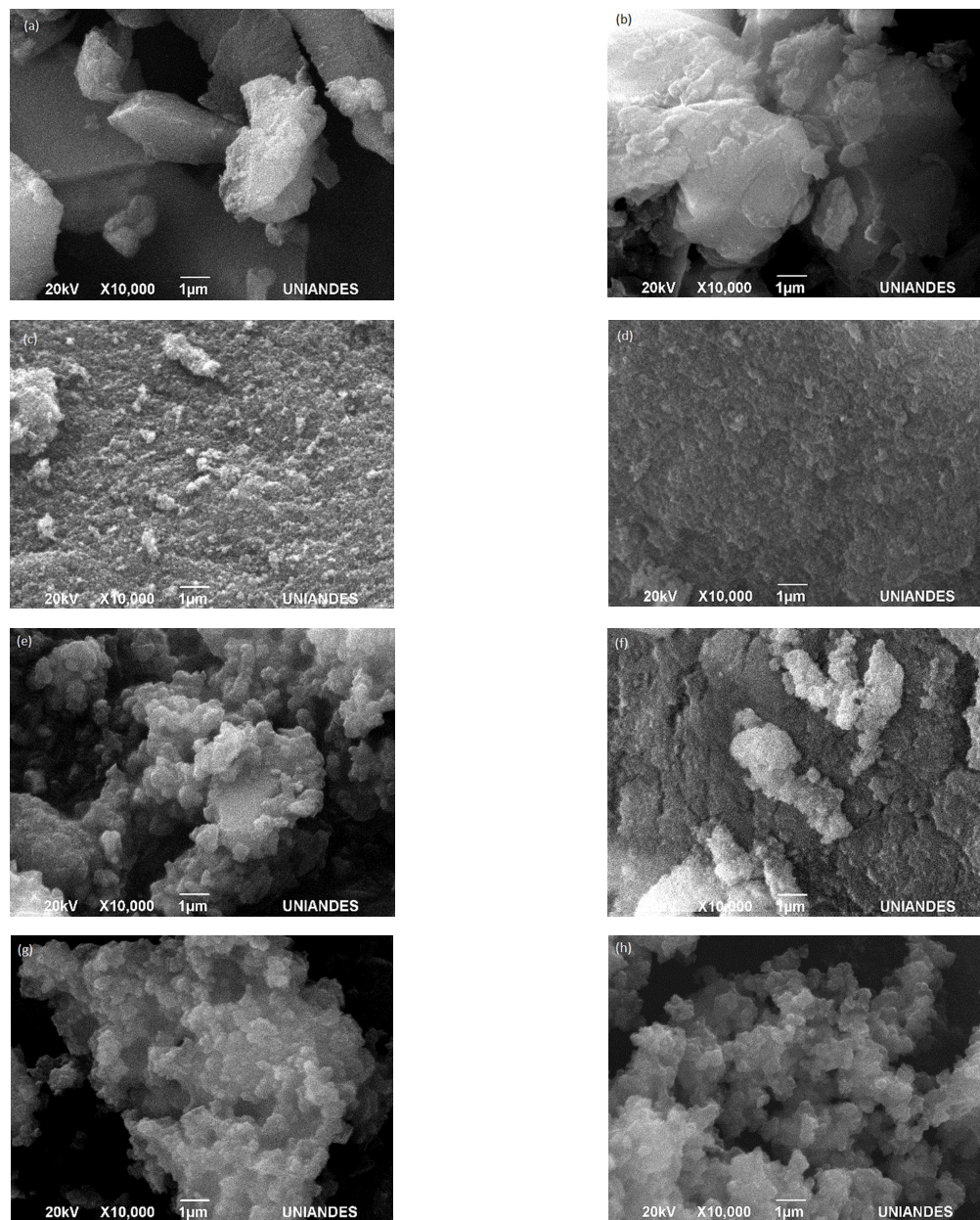


Figure 4. Scanning electron microscopy: (a) AeW25; (b) AeW50; (c) AeW100; (d) AeW200; (e) AeW400; (f) AeW600; (g) AeW800 and (h) AeW1500.

The method QSDFT, presents significant advances over traditional DFT method, assumes that the pore walls are homogeneous such as planes graphite. On the one hand, this approach offers flexibility in describing the boundary between the fluid-solid by varying the density of the solid, and the surface thickness of the diffuse solid layer. In addition, the QSDFT model offers an additional advantage over the NLDFT model, due to the computational ease, since it can consider a density distribution on a one-dimensional solid, where the effects of roughness and surface heterogeneity are considered. The theoretical bases corresponding to QSDFT model are developed in different works of Ravikovitch and Neimark [33-34]. The detailed description the QSDFT model application, for micro-mesoporous carbon is described in [36]. In summary, what can be said is that the surface obtained in general for both series I and series II, correspond to nonhomogeneous and

rough geometric surfaces that are the foundations in which the QSDFT model was developed [33-36].

Figure 2d shows the nitrogen adsorption-desorption isotherms of N_2 to $-196^\circ C$ for the series II: AeW400, AeW600, AeW800 and AeW1500. It is observed, that they are similar and correspond to Type I isotherms combined with those of type IV, in accordance with [20,22,46], that fit also to the recent recommendations suggested by the IUPAC [46]. The hysteresis loop is submitted to different ranges of relative pressure, according to the samples of aerogels thus: samples AeW400, AeW600 and AeW800 to relatively high pressures (0.4 to 1.0) and the sample AeW1500 to pressures of (0.1 to 0.9), which shows the development of mesopores, when using these relations of Na_2CO_3 as a catalyst during the synthesis of aerogel. This may be due to the formation of aggregates in the time of polymerization according to the number of monomers

initially formed by the action of the amount of catalyst on the resorcinol.

It is interesting to note that these relations of R/C (400, 600, 800 and 1500) is where presents the development of mesopores. This is associated with the polymerization mechanism between the resorcinol and sodium carbonate; a careful examination of the isotherms of adsorption of N₂ at -196 °C, clearly show that the isotherm AeW800 has the wider hysteresis loop, which corroborates the view the volume of mesopores that develops this aerogel. Table 1, shows that the volumes of mesopores calculated using the method BJH are on the increase: AeW400 (0.18 cm³/g), AeW600 (1.23 cm³/g), AeW800 (1.28 cm³/g) and finally, in the sample AeW1500 decays (0.31 cm³/g). This is associated with a possible collapse of the structure, developed by effect of the excess catalyst during the process of adding prior to the polymerization, and the subsequent pyrolysis crushing some bridges of the internal structure. The volume of micropores developed was calculated using the same methods above, taking values from 0.36 to 1.35 cm³/g taking as a model of pore cylinder-slit and using the QSDFT. However, for the aerogel AeW1500 value decreases to 0.61 cm³/g, which as explained before this is associated with the process of polymerization. In this series II aerogels to these relations R/C also increases continuously its surface area specifics.

In Figure 3a comparative study of the experimental data is presented versus the NLDFT and QSDFT models, applying the model of pore size cylindrical-slit form. This kernel considers the heterogeneity and roughness of the surface of the carbonaceous structures in this case of the carbon aerogel and allow obtain a pore size distribution, more reliable, as found in this research [33,34].

The adjustments show that using the algorithm QSDFT applying the model cylinder-slit is that fits better, and this is in good agreement with the results obtained experimentally with the isotherms of N₂ to -196 °C and that it have been extensively analysed in this work. This shows that the pores of these materials are rough and heterogeneous type. Additionally, as seen in Figure 3, the model QSDFT shows a better description of the PSD, where it is possible detect the development of microporosity narrow.

The results discussed in this research are in good agreement with the scanning electron micrographs, where with a magnification of 10.000 it is possible see as with R/C increases, the particle size increases which is directly related to what explained above with the synthesis process aerogel resorcinol/formaldehyde (Figure 4).

It is evident that in the measure that the relation R/C increases, the formation of structural aggregates is incremented being clearer, allowing to deduce that the higher amount of catalyst more monomeric units are formed and therefore the formation of structural units it becomes greater, resulting in some structure pearl necklace type characteristics of these materials.

4. Conclusion

In this work, carbon aerogel were prepared, and studied the effects in a wide range of R/C ratio on texture function. The results show that the increase in the R/C ratio generates two series of aerogels: one series produces microporous materials, and a second series characterized by the development of mesoporosity. It is probable that these differences, that give rise to the development of mesoporosity in series II are due to the reaction between resorcinol and Na₂CO₃ in the first stage, corresponding to the addition of formaldehyde to form the monomer. After applying various models, the best fit was obtained for the QSDFT model for a porous system of cylinder-slits. The specific surface areas obtained, ranged from 64 to 990 m²/g. D-A and BJH models contribute important information about the characteristics of aerogel texture. The struc-

tures in the materials obtained are basically heterogeneous with an increased width distribution and pore volumes suitable for using these materials in various applications.

Acknowledgements

The authors are thankful to the existing framework agreement between Guajira University, the National University of Colombia and the Andes University (Bogota, Colombia). In addition, want to give special thanks to the Grant Basic Sciences by the University of the Andes through the Faculty of Science and the Vice-rectory of Research. The authors also wish to thank the Bank of the Republic of Colombia for their funding and the Convention 3580 and its financial support that helped to make this research possible.

References

- Zarzycki, J.; Woignier, T. *Aerogels*, Springer Proceedings in Physics 6th, Springer-Verlag Berlin Heidelberg, 1986.
- Pekala, R. W.; Alviso, C. T. *Mater. Res. Soc. Symp. Proc.* **1992**, *270*, 3-14.
- Pekala, R. W.; Alviso, C. T.; Kong, F. M.; Hulsey, S. S. *J. Non-Cryst. Solids* **1992**, *145*, 90-98.
- Pekala, R. W.; Kong, F. M. *Polym. Prepr.* **1989**, *30*, 221-223.
- Lin, C.; Ritter, J. A. *Carbon* **1997**, *35*, 1271-1280.
- Gallegos, S. E.; Perez, C. A. F.; Maldonado, H. F. J.; Carrasco, M. F. *Chem. Eng. J.* **2012**, *181-182*, 851-855.
- Luzny, R.; Ignasiak, M.; Walendzewski, J.; Stolarski, M. *Chemik* **2014**, *68(6)*, 544-553.
- Nianping, L.; Jun, S.; Pung, L. *Microporous Mesoporous Mater.* **2013**, *167*, 176-181.
- Yonk, K.; Ya, Z.; Xiaodong, S.; Sheng, C.; Meng, Y.; Kaming, T.; Junjun, Z. *J. Non-Cryst. Solids* **2012**, *358*, 3150-3155.
- Yousheng, T.; Morinobu, E.; Katsumi, K. *Recent Pat. Chem. Eng.* **2008**, *1*, 192-200.
- Ai, D.; Bin, Z.; Zhihua, Z.; Jun, S. *Materials* **2013**, *6(3)*, 941-968.
- Al-Muhtaseb, S. A.; Ritter, J. A. *Adv. Mater.* **2013**, *15(2)*, 101-114.
- Jyotsna, G.; Kadirvelu, K.; Rajagopal, C.; Garg, V. K. *Ind. Eng. Chem. Res.* **2006**, *45*, 6531-6537.
- Gang, P. W.; Junbing, Y.; Dapeng, W.; Rui, X.; Khalil, A.; Chun, X. L. *Mater. Lett.* **2014**, *115*, 1-4.
- Kaneko, K.; Ishii, C. *Colloids Surf.* **1992**, *67*, 203-212.
- Kaneko, K.; Shimizu, K.; Suzuki, T. *J. Chem. Phys.* **1992**, *98*, 8705-8711.
- Setoyama, N.; Kaneko, K.; Rodriguez, R. F. *J. Phys. Chem.* **1996**, *100*, 10331-10336.
- Setoyama, N.; Ruike, M.; Kasu, T.; Suzuki, T.; Kaneko, K. *Langmuir* **1993**, *9(10)*, 2612-2617.
- Setoyama, N.; Suzuki, S.; Kaneko, K. *Carbon* **1998**, *36*, 1459-1467.
- Ruike, M.; Kasu, T.; Setoyama, N.; Suzuki, T.; Kaneko, K. *J. Phys. Chem.* **1994**, *98(38)*, 9594-9600.
- Liyama, T.; Nishikawa, K.; Otowa, T.; Kaneko, K. *J. Phys. Chem.* **1995**, *99(25)*, 10075-10076.
- Sing, K. S. W.; Everett, D. H.; Haul, R. A. W.; Moscou, L.; Pierotti, R. A.; Rouquerol, F.; Siemieniewska, T. *Pure Appl. Chem.* **1985**, *57(4)*, 603-619.
- Hanzawa, Y.; Kaneko, K.; Pekala, R. W.; Dresselhaus, M. S. *Langmuir* **1996**, *12(26)*, 6167-6169.
- Dollimore, D.; Heal, G. R. *J. Appl. Chem.* **1964**, *14*, 109-114.
- Dollimore, D.; Heal, G. R. *J. Colloid Interface sci.* **1979**, *33*, 508-519.
- Pekala, R. W.; Schaefer, D. W. *Macromolecules* **1993**, *26*, 5487-5493.
- Schaefer, D. W.; Pekala, R. W.; Beaucage, G. *J. Non-Cryst. Solids* **1995**, *186*, 159-167.
- Maldonado, H. F. *J. Catal. Today* **2013**, *218-219*, 43-50.
- Morales, T. S.; Maldonado, H. F. J.; Pérez, C. A. F.; Carrasco, M. F. *Phys. Chem. Chem. Phys.* **2012**, *12*, 10365-10372.
- Fairen, J. D.; Carrasco, M. F.; Moreno, C. C. *Carbon* **2006**, *44*, 2301-2307.
- Barret, E. P.; Joyner, L. G.; Halenda, P. P. *J. Am. Chem. Soc.* **1951**, *73*, 373-380.
- Dubinin, M.; Astakhov, V. A. *Bull. Acad. Sci. USSR, Div. Chem. Sci.* **1971**, *20*, 3-7.
- Ravikovitch, P. I.; Neimark, A. V. *Langmuir* **2006**, *22*, 11171-11179.
- Neimark, A. V.; Lin, Y.; Ravikovitch, P. I.; Thommes, M. *Carbon* **1998**, *36*, 469-474.
- Ravikovitch, P. I.; Vishnyakov, A.; Russo, R.; Neimark, A. V. *Langmuir* **2000**, *16(5)*, 2311-2320.
- Neimark, A. V.; Ravikovitch, P. I.; Vishnyakov, A. *J. Phys. Condens. Matter* **2003**, *15*, 347-365.
- Fonseca-Correa, R. A.; Giraldo, L.; Moreno-Piraján, J. C. *Microporous Mesoporous Mater.* **2017**, *248*, 164-172.
- Brunauer, S.; Emmett, P. H. *J. Am. Chem. Soc.* **1935**, *57*, 1754-1755.

- [39]. Brunauer, S.; Emmett, P. H. *J. Am. Chem. Soc.* **1937**, *59*, 2682-2689.
- [40]. Brunauer, S.; Emmett, P. H.; Teller, E. *J. Am. Chem. Soc.* **1938**, *60*, 309-319.
- [41]. Brunauer, S.; Deming, L. S.; Deming, W. E. Teller, E. *J. Am. Chem. Soc.* **1940**, *62*, 1723-1732.
- [42]. Vargas, D. D. P.; Giraldo, L.; Moreno, P. J. C. *Eur. J. Chem.* **2017**, *8*(2), 130-136
- [43]. Elrazek, H. J. A.; Abd, E. D. R.; Rashad, A. M.; Elazab, W.; Fathy, A. H. *Eur. J. Chem.* **2015**, *6*(4), 488-492
- [44]. Dubinin, J. M. M. *Prog. Surf. Membr. Sci.* **1975**, *9*, 1-70
- [45]. Thommes, M.; Cychoz, K. A.; Neimark, A. V. *Novel carbon adsorbents*, 1st edition, Elsevier, **2012**.
- [46]. Thommes, M.; Kaneko, K.; Neimark, A. V.; Olivier, J. P.; Rodriguez, R. F.; Rouquerol, J.; Sing, K. S. W. *Pure Appl. Chem.* **2015**, *87*, 1051-1069.